NEUROSCIENCE
RESEARCH ARTICLE

B. S. Heit et al. / Neuroscience 461 (2021) 102–117

Synaptic and Network Contributions to Anoxic Depolarization in Mouse Hippocampal Slices

Bradley S. Heit,[a,b] Patricia Dykas,[b] Alex Chu,[b] Abhay Sane[b] and John Larson[b]*

[a] *Graduate Program in Neuroscience, University of Illinois at Chicago, Chicago, IL 60612, United States*

[b] *Department of Psychiatry, University of Illinois at Chicago, Chicago, IL 60612, United States*

Abstract—Ischemic stroke remains the third leading cause of death and leading cause of adult disability worldwide. A key event in the pathophysiology of stroke is the anoxic depolarization (AD) of neurons in the ischemic core. Previous studies have established that both the latency to AD and the time spent in AD prior to re-oxygenation are predictors of neuronal death. The present studies used hippocampal slices from male and female mice to investigate the electrophysiological events that affect latency to AD after oxygen deprivation. The results confirm that the epoch between AD and re-oxygenation largely determines the magnitude of synaptic recovery after anoxic challenge. Using a selective antagonist of adenosine A_1 receptors, we also confirmed that adenosine released during anoxia (ANOX) suppresses synaptic glutamate release; however, this action has no effect on AD latency or the potential for post-anoxic recovery of synaptic transmission. In contrast, antagonism of AMPA- and NMDA-type glutamate receptors significantly prolongs the latency to AD and alters the speed and synchrony of associated depolarizing waves. Experiments using slices with fields Cornu ammonis 3 (CA3) and Cornu ammonis 1 (CA1) disconnected showed that AD latency is longer in CA1 than in CA3; however, the early AD in CA3 is propagated to CA1 in intact slices. Finally, AD latency in CA1 was found to be longer in slices from female mice than in those from age-matched male mice. The results have implications for stroke prevention and for understanding brain adaptations in hypoxia-tolerant animals.

Key words: anoxic depolarization, glutamate excitotoxicity, hypoxia, ischemia.

INTRODUCTION

Ischemic stroke is the third leading cause of death worldwide, and a primary contributor to death and disability in both developing and developed countries (Burke et al., 2012). On average, someone in the United States suffers an ischemic stroke every 40 s and dies from one approximately every 4 min (Benjamin et al., 2018). The loss of blood supply to brain tissue (ischemia) and consequent depletion of ATP induces a rapid cascade of reactions that leads to neuronal death beginning within minutes and continuing for hours and days thereafter. Much of what is known about the neuronal responses to stroke has been learned from studies of brain slices or isolated neurons in primary culture *in vitro* after exposure to total (anoxia) or partial (hypoxia) oxygen deprivation. The initial events proceed as follows (Lipton, 1999): Oxygen or combined oxygen/glucose deprivation leads to ATP depletion, that may produce a very transient initial membrane hyperpolarization due to opening of ATP-dependent K^+ channels. ATP breakdown leads to a build-up of adenosine that is released into the extracellular compartment, binding to presynaptic A_1 receptors which partially antagonize synaptic glutamate release. The rundown of membrane pumps in the absence of ATP causes the neurons to slowly depolarize, leading to synaptic release of glutamate and, with further depolarization, the release of glutamate from reverse operation of glutamate transporters (Rossi et al., 2000), which synergize with K^+ efflux to massively depolarize the cells.

*Corresponding author. Address: Psychiatric Institute (M/C 912), University of Illinois at Chicago, 1601 W. Taylor Street, Chicago, IL 60612, United States.
E-mail address: jrlarson@uic.edu (J. Larson).

Abbreviations: 8-PT, 8-phenyltheophylline; ACSF, Artificial cerebral spinal fluid; AD, Anoxic depolarization; Amp, Amplitude; AMPA, α-amino-3-hydroxy-5-methyl-4-isoxazolepropionic acid; Anova, Analysis of variance; ANOX, Anoxia; ANTI, Antidromic; AS, Antidromic spike; CA1, Cornu ammonis 1; CA3, Cornu ammonis 3; CNQX, 6-cyano-7-nitroquinoxaline-2,3-dione; CPX, 8-cyclopentyl-1,3-dipropylxanthine; CPT, 8-cyclopentyltheophylline; D-AP5, D-2-amino-5-phosphonopentanoic acid; DC, Direct current; DG, Dentate gyrus; DMSO, Dimethyl sulfoxide; EAAC, Excitatory amino acid carrier; EEG, Electroencephalogram; EPSC, Excitatory postsynaptic current; fEPSP, Field excitatory postsynaptic potential; IPI, Inter-pulse intervals; MRI, Magnetic resonance imaging; NMDAR, N-methyl-D-aspartate receptor; OGD, Oxygen glucose deprivation; PPF, Paired pulse facilitation; PRE, Pre oxygen deprivation; PYR, *Stratum pyramidale*; RAD, *Stratum radiatum*; REC, Recovery; SEM, Standard error of mean; SYN, Synaptic; t-PA, Tissue plasminogen activator; TTX, Tetrodotoxin.

https://doi.org/10.1016/j.neuroscience.2021.02.021
0306-4522/

These ischemia-driven reactions ultimately result in the loss of membrane potentials, or anoxic depolarization (AD), in affected neurons. Importantly, it has become widely-accepted that the AD event is the spark that ignites the neurotoxic cascade leading to cell death (Ayata, 2018; Hartings et al., 2017; Leao, 1947). Both the latency to AD and the time remaining in AD prior to re-oxygenation are important for the extent of cell damage in ischemia: shorter AD latencies lead to greater cell death while shorter delays between AD and re-oxygenation lead to greater survival (Jarvis et al., 2001; Kaminogo et al., 1998; Kostandy, 2012).

The fact that certain brain regions are selectively vulnerable to ischemic damage implies that there may be factors inherent either in the neurons themselves or in the networks in which they reside that influence the extent or rapidity with which they respond to metabolic insults. Cornu ammonis 1 (CA1) neurons in the hippocampus are particularly sensitive to ischemia, as they are the first to die after global ischemia in the brain (Schmidt-Kastner and Freund, 1991). For isolated neurons, AD may be directly related to the effects of metabolic inhibition on membrane ion pumps. However, the situation is more complicated *in vivo* and in slices since neurons in intact networks are affected by glutamate and potassium released from neighboring neurons and may be affected by synaptic connections with more distant neurons.

In addition, studies of animals which live in chronically hypoxic environments or experience hypoxia intermittently show that isolated brain slices from these animals take longer to undergo AD than slices from appropriate comparison species (Geiseler et al., 2016; Larson et al., 2014; Larson and Park, 2009). The contributions of individual steps in the anoxic cascade to the overall AD latency in these hypoxia-tolerant animals or, indeed, in typical laboratory rodents are not well understood. The present work was undertaken to examine which of the steps can be modified to extend AD latency in order to identify targets for investigation in hypoxia-tolerant animals that may represent putative therapeutic approaches for stroke.

Experiments were designed to investigate local synaptic and network factors that influence the latency to AD in the CA1 field of mouse hippocampal slices *in vitro*. Slices were maintained in an interface-type chamber design in which oxygen deprivation alone is used to model ischemia and produces rapid AD similar to that which occurs in stroke (Croning and Haddad, 1998). The results indicate that (1) while adenosine release and action on A_1 adenosine receptors antagonize synaptic glutamate release during anoxic challenge, it has no significant effect on the latency to AD; (2) antagonism of NMDA- and AMPA-type glutamate receptors prolongs the latency to AD; (3) neurons in field Cornu ammonis 3 (CA3) show AD earlier than those in CA1 when the two regions are disconnected; however the early AD in CA3 is propagated from the CA3 network to CA1 in intact slices; and (4) slices from female animals show delayed AD relative to those from males.

EXPERIMENTAL PROCEDURES

Animals

Most experiments were performed using 2–4 month old male CD-1 mice acquired from Charles River Laboratories (Wilmington, MA). Two experiments used C57Bl/6 (B6) mice obtained from Jackson Laboratories (Bar Harbor, ME). One experiment used B6 mice (2–4 months old) to examine the electrophysiological recovery of slices re-oxygenated at varying times after AD. A second experiment used B6 mice (8–9 months old) to examining sex differences in anoxia sensitivity. All efforts were made to maximize use of mice available in our colonies. The two datasets from B6 mice are noted in the figure legends. All experiments were conducted in accordance with National Institutes of Health guidelines and were approved by the Animal Care Committee of the University of Illinois at Chicago.

Electrophysiology

Transverse hippocampal slices were prepared in the conventional manner (Larson et al., 1999; Larson and Park, 2009). Briefly, mice were decapitated and the brain rapidly excised. Anesthetic was not administered as it can alter subsequent anoxia tolerance in slices (Bickler et al., 2005). The hippocampus was dissected free, and slices cut on a tissue chopper at 400 μm transverse to the long axis. Slices were then maintained in an interface chamber at 34 °C, with the upper surfaces of slices exposed to an atmosphere of carbogen gas (95% O_2, 5% CO_2) and continually perfused (1 mL/min) underneath with artificial cerebrospinal fluid (ACSF) containing (in mM): NaCl 124, KCl 3.0, KH_2PO_4 1.0, $NaHCO_3$ 26, $MgSO_4$ 2.5, $CaCl_2$ 3.4, D-glucose 10, sodium-L-ascorbate 1.9 (unless specified otherwise), saturated with carbogen. The gas supplied to the chamber atmosphere flowed at a rate of 1 L/min.

Recordings were made with glass micropipettes filled with 2 M NaCl (1–5 MΩ). Field excitatory postsynaptic potentials (fEPSPs) were evoked in CA1 by stimulation of Schaffer/commissural fibers in *stratum radiatum* of subfield CA1c (near the border of CA3) and recorded in *s. radiatum* of field CA1b. Antidromic spikes (ASs) in CA1 were induced by stimulation of the alveus in subfield CA1a (near the subiculum) and recorded in *s. pyramidale* of subfield CA1b. fEPSPs in CA3 were evoked by stimulation in *s. radiatum* of CA3a and recorded in the same layer of CA3b. In some experiments, a No. 10 scalpel blade was used to separate the CA3 region from CA1 before placement into the interface chamber.

Evoked responses were amplified (100–500×), filtered (bandpass 0.1 Hz–5 KHz), digitized by microcomputer (PC), and analyzed on-line using custom software. Responses (fEPSPs or ASs) were evoked at 20-s intervals throughout the experiments. Baseline stimulus intensity was set to evoke a half-maximal fEPSP in each slice. Baseline recordings were taken for at least 10 min prior to manipulations. Initial slope and

peak amplitude were calculated for each fEPSP and normalized to the baseline average in each slice. ASs were quantified as the peak amplitude of the negative spike from the post-stimulus baseline. In some experiments, paired-pulse facilitation (PPF) was assessed using stimuli separated by 75 ms. In these cases, PPF was determined as the percent increase in the amplitude of the second response relative to the amplitude of the first response in the pair.

Anoxia

For ‘‘anoxia” experiments, all O_2 in the atmosphere in the chamber above slices and in the perfusion ACSF was replaced with N_2. We refer to this condition as ‘‘nominal anoxia” as the slice chamber is an open system, potentially contaminated with trace O_2 from the outside air. In these experiments, nominal anoxia was maintained until slices displayed AD, signaled by the loss of synaptic response, a large, slow shift in the field potential (‘‘the AD wave”), and abolition of the presynaptic fiber volley (see Fig. 1). We chose to use the term ‘‘AD wave” rather than the ‘‘DC shift” used by others since our recordings were not strictly DC-coupled. Given the coincidence of the field potential shift, the loss of the fiber volley, and the loss of the AS (when available), the AD wave is undoubtedly equivalent to the DC shift. The AD wave was observed using an oscilloscope and its latency from anoxia onset (i.e. ‘‘AD Latency”) was recorded with a stopwatch. For all experiments, the ‘‘anoxic period” refers to the epoch starting from the replacement of O_2 with N_2 (anoxia) to complete re-oxygenation, which includes the duration of time slices were left in the depolarized state after AD. In some experiments, the field potential was continuously recorded by computer (digitized at 100 Hz) throughout experiments to display the AD waves in figures along with evoked field potentials. In these cases, the AD onset was taken to be the time when the first digitized point had a negative voltage greater than −0.25 mV and the AD end was taken to be the time point after the AD peak when the negative wave reached −0.25 mV. The AD wave amplitude was measured as the peak negativity while the AD wave duration was measured as the difference between AD wave onset and end (see Fig. 1). After a defined time period elapsed after the AD (varied in different experiments), slices were re-oxygenated (replacement of N_2 with O_2) and recordings continued for 30–45 min to examine extent of recovery of evoked field potentials.

Hypoxia

‘‘Partial hypoxia” was induced by replacing the O_2 content of the chamber atmosphere and perfusion ACSF with varying concentrations of N_2 (Fowler, 1993; Larson and Park, 2009) for a 15- or 30-min time period. In these cases, the % O_2 content refers to the proportion of the non-CO_2 component of the gas supply (CO_2 was always maintained at 5%). For normoxia, the non-CO_2 component was 100% O_2; for 25% O_2, this component was 25% O_2 and 75% N_2. The percent change in fEPSP amplitude at the end of the hypoxia period was taken as the acute response to hypoxia, and the degree of recovery after reinstatement of 100% O_2 was determined after 30–60 min as previously described (Larson and Park, 2009). No slices were exposed to more than one episode of hypoxia or anoxia. This is important because anoxia exposure may inflict irreversible damage or produce a ‘preconditioning’ or protective effect on surviving neurons (Schurr et al., 1986).

Drugs

All drugs were obtained from Tocris Bioscience (Bio-Techne, Minneapolis, MN). The adenosine A_1 receptor antagonist, 8-cyclopentyl-1,3-dipropylxanthine (CPX), was dissolved in 100% DMSO at 10 mM and diluted in ACSF to final concentrations of 10–1000 nM. The AMPA receptor antagonist, 6-cyano-7-nitroquinoxaline-2, 3-dione (CNQX) was dissolved in 100% DMSO at 50 mM and diluted in ACSF to a final concentration of 50 μM. The NMDA receptor antagonist, D-2-amino-5-phosphonopentanoic acid (AP5) was dissolved in water at 50 mM and diluted in ACSF to a final concentration of 250 μM.

Statistics

Data are presented as mean ± SEM. Statistical analyses were conducted using Graphpad Prism (v. 8). Unpaired or paired *t*-tests were used for comparisons of two groups run independently or as paired comparisons, respectively. Analysis of variance (Anova) was used for tests involving more than two groups. Dunnett’s or Sidak’s tests were used for multiple comparisons if the overall Anova was significant. Slice schematics were generated using BioRender (biorender.com) software.

RESULTS

Anoxia induces rapid loss of synaptic and action potentials and a depolarizing wave that originates in the dendrites and propagates to the soma

Fig. 1 shows the positioning of electrodes as well as recordings of synaptic potentials in the dendritic layer (*stratum radiatum*) and antidromic potentials in the cell body layer (*s. pyramidale*) before, during, and after a brief episode of oxygen deprivation (nominal anoxia). Synaptic (Fig. 1B) and antidromic (Fig. 1C) responses were recorded alternately at 10 s intervals throughout the experiment. After a baseline period of at least 10 min in normoxic conditions (95% O_2/5% CO_2), the slice was exposed to the anoxic condition (95% N_2/5% CO_2). After about one minute, the synaptic response began to decline while the antidromic response was maintained for about another minute, after which it decreased and disappeared within about 40 s, roughly coincident with the loss of the fiber volley and the synaptic response (Fig. 1D). Continuous recordings at the synaptic and antidromic recording sites showed that a large, negative extracellular slow wave (DC shift) occurred simultaneously with the loss of evoked potentials, although slightly earlier in the dendritic layer

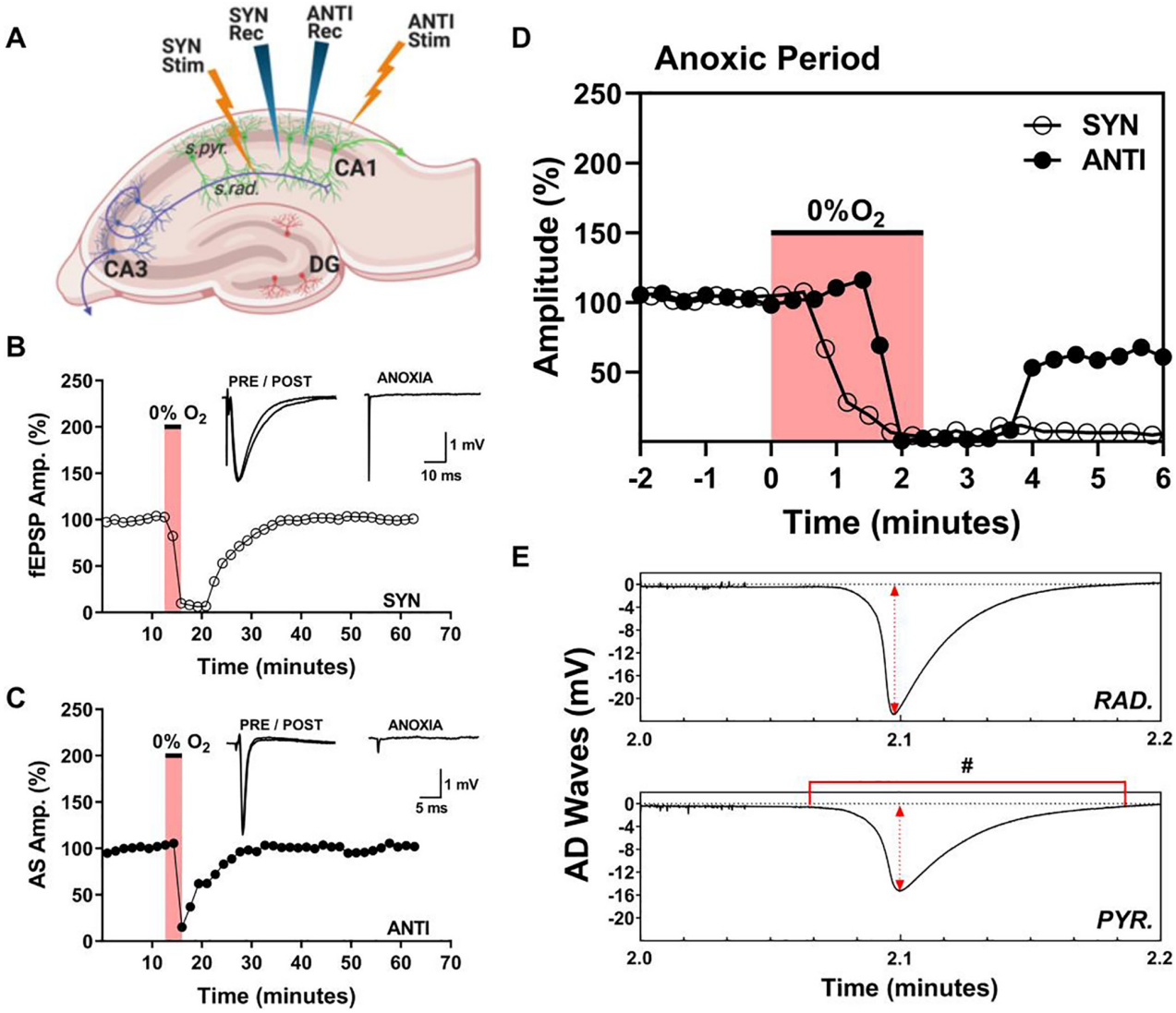

Fig. 1. Effects of anoxia on evoked potentials and spontaneous electrical activity in the mouse hippocampal slice. **(A)** Schematic of synaptic organization in the hippocampal slice and placement of synaptic (SYN) and antidromic (ANTI) stimulating and recording electrodes. **(B, C)** Graphs show normalized measurements of synaptic (fEPSP Amp.) responses **(B)** and antidromic spikes (AS Amp.) response **(C)** before, during, and after an episode of anoxia. Each circle represents the average amplitude of five consecutive responses, normalized to the pre-anoxia baseline average. Synaptic and antidromic responses were evoked alternately at 10 s intervals. The pink area denotes the anoxic period, and the insets show individual evoked responses for the pre-anoxic (PRE; immediately prior to anoxia), anoxic (ANOX; last trial before re-oxygenation), and recovery (POST; 45 min after re-oxygenation) periods for synaptic and antidromic responses. The anoxic period was terminated by the appearance of the AD (see text). **(D)** The expanded anoxic period graph illustrates changes in antidromic and synaptic responses with greater temporal resolution. The abscissa shows time relative to anoxia onset. Each point represents a single evoked response on the synaptic (open circles) or antidromic (closed circles) pathway. Note that the synaptic response began to decrease about one min before the antidromic response. **(E)** Segments of continuous recordings at the synaptic recording site in *s. radiatum* (*RAD*) and the antidromic recording site in *s. pyramidale* (*PYR*) showing the large, negative potential (“AD wave”) that occurred nearly simultaneously at the two sites and contemporaneous with the loss of the antidromic response and the fiber volley at the synaptic recording site. The synaptic response (fEPSP) had decreased significantly before the appearance of AD waves. The AD wave recorded in the apical dendritic layer preceded the AD wave recorded in the somatic layer by a few seconds. The times of AD wave peaks are indicated by arrows. The time period used to calculate AD wave duration is marked by the horizontal bar in the lower panel #. Time axis relative to anoxia onset as in **(D)**. (For interpretation of the references to colour in this figure legend, the reader is referred to the web version of this article.)

than in the somatic layer (Fig. 1E). The slow wave in the field potential has been described previously and identified with a large intracellular depolarization in individual pyramidal neurons (Arai et al., 1990). Therefore, it will be referred to as the anoxic depolarization wave (“AD wave”) in this and subsequent figures. The AD wave was usually preceded by several seconds of increased spontaneous neuronal spiking consistent with a slowly-developing depolarization. The slice was re-oxygenated (95% O_2/5% CO_2) immediately after detection of the AD and both synaptic transmission and ASs fully recovered within 15 min. Similar results were seen in nine slices. In all cases, the synaptic response declined prior to any effect on the antidromic response and the AD

wave in the dendritic layer (*s. radiatum*) always preceded the AD wave in the somatic layer (*s. pyramidale*) (mean difference: 1.67 sec ± 0.44, paired $t_8 = 3.78$, $p = 0.0054$). Aside from the consistent difference in AD latency, paired analyses showed no differences between dendritic and somatic AD wave peak amplitude (*RAD*: 13.6 ± 2.7, *PYR*: 12.4 ± 2.1 mV, paired $t_8 = 1.03$, $p = 0.33$) or AD wave duration (*RAD*: 8.0 ± 1.0, *PYR*: 8.7 ± 1.0 s, paired $t_8 = 1.51$, $p = 0.17$), although some experiments showed slight within-slice variance.

Duration in the depolarized state after AD determines extent of recovery

The effect of the time spent in the depolarized state between AD and re-oxygenation ('delay after AD') on recovery of synaptic transmission is shown in Fig. 2. After a 10-minute baseline, slices were exposed to anoxic conditions until AD occurred, and then re-oxygenated after delays ranging from 0 to 300 sec. The delay used in each slice was randomly determined. Recovery of synaptic transmission was measured 30 min after re-oxygenation. Immediate re-oxygenation (Fig. 2A) resulted in 100% recovery, a delay of 2 min after AD led to partial recovery (Fig. 2B), and re-oxygenation after a delay of 5 min (Fig. 2C) failed to induce any recovery of the synaptic response. Analysis of variance on data from a total of 57 experiments with 7 different delays (Fig. 2D) showed a highly significant effect of delay on recovery ($F_{6,50} = 15.06$, $p < 0.0001$); all delays longer than 60 s showed poorer recovery than immediate re-oxygenation. Latencies to AD in these experiments ranged from 90 to 360 s, but did not differ (by design) in groups subject to different delays before re-oxygenation ($F_{6,50} = 2.16$, $p = 0.063$). These results are in agreement with earlier reports showing that time in the depolarized state is a strong determinant of post-anoxic recovery (Balestrino et al., 1989; Balestrino and Somjen, 1986; Pérez-Pinzón et al., 1998).

Attenuation of synaptic transmission by partial hypoxia is mediated by adenosine release acting on presynaptic A_1 receptors

As shown above (Fig. 1), the first effect of nominal anoxia is a suppression of synaptic transmission that occurs prior to any effect on the AS. Previous studies have established that oxygen deprivation leads to the build-up and release of adenosine; extracellular adenosine acts on presynaptic A_1 receptors to suppress glutamate release (Arlinghaus and Lee, 1996; Croning et al., 1995; Dunwiddie and Masino, 2001; Fowler, 1989) by inhibiting presynaptic calcium channels (Gundlfinger et al., 2007). However, whether or not the released adenosine protects against anoxic damage by delaying AD or antagonizing excitotoxic damage is a matter of debate (Fowler, 1990; Fusco et al., 2018; Lee and Lowenkopf, 1993; Pearson et al., 2006). In order to examine this issue, we first verified that a potent and selective antagonist of adenosine A_1 receptors, 8-cyclopentyl-1,3 dipropylxanthine (CPX), blocks hypoxia-induced suppression of synaptic transmission. Since nominal anoxia rapidly leads to AD, we used a moderate hypoxia paradigm to induce a graded synaptic response (Fowler, 1993; Larson and Park, 2009). Lowering the non-CO_2 component of the chamber atmosphere and gas bubbling the ACSF from 100% O_2 to 25% O_2 (75% N_2) resulted in a ~50% suppression of synaptic responses (Fig. 3A) and an increase in paired-pulse facilitation (Fig. 3B), consistent with a presynaptic mechanism (Coelho et al., 2000). This was confirmed by the lack of effect of hypoxia on ASs (Fig. 3C, D). CPX showed a dose-dependent antagonism of the hypoxia-induced synaptic suppression, with a threshold effect at 30 nM and complete preservation of the synaptic response at 300 and 1000 nM (Fig. 4).

Antagonism of adenosine A_1 receptors delays the attenuation of synaptic transmission induced by anoxia but has no effect on the latency to AD or recovery of synaptic transmission after re-oxygenation

Antagonists of adenosine A_1 receptors are variously reported to prevent AD (Pearson et al., 2006), delay its occurrence (Fusco et al., 2018), shorten its latency (Lee and Lowenkopf, 1993), or have no effect (Fowler, 1990; Oyama et al., 2020). We treated slices with CPX (300 nM) or DMSO vehicle for at least 30 min before an episode of nominal anoxia. Anoxia was maintained until AD occurred and then continued for a two-minute period after AD; slices were then re-oxygenated and monitored for a 30-minute recovery period. The two-minute period after AD before re-oxygenation was selected, based on data in Fig. 2, to allow detection of a drug effect on either suppression or enhancement of recovery. The drug (CPX) or sham (vehicle) treatments were maintained through the recovery period. Fig. 5(A, B) shows representative experiments for each condition. Both the sham and CPX-treated slices showed a rapid loss of synaptic transmission in anoxia, with AD in the control slice after 130 sec and after 142 sec in CPX. Both slices recovered to a steady state level of synaptic transmission about half of that before the episode of anoxia. The data for all experiments with high temporal resolution during the anoxic period (Fig. 5C) show that the suppression of synaptic transmission was delayed by about one minute in CPX-treated slices. However, comparison of AD latencies (Fig. 5D) and extent of recovery (Fig. 5E) showed no significant differences between CPX- and vehicle-treated slices.

Pharmacological antagonism of glutamate receptors delays AD

The lack of effect of CPX on AD latency was surprising since adenosine A_1 receptors clearly suppress evoked glutamate release during the initial response to anoxia (Fig. 5C) and activation of glutamate receptors is implicated in hypoxia-induced cell death. On the other hand, evidence that blockade of glutamate receptors affects AD latency in hippocampal slices is sparse (Aitken et al., 1988; Fusco et al., 2018; Roberts et al., 1998). We investigated the contribution of glutamate receptors by perfusing slices with a cocktail containing

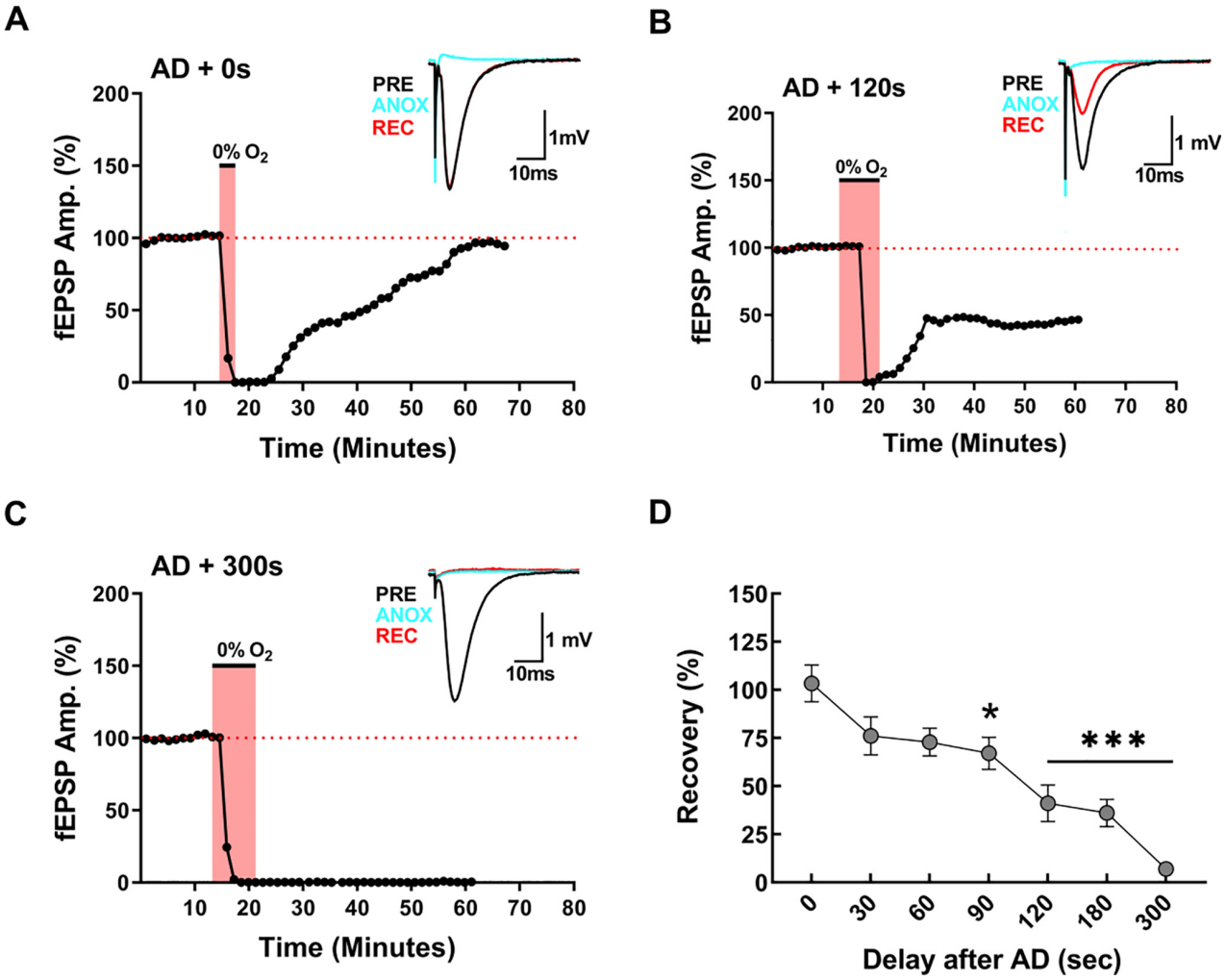

Fig. 2. Duration in depolarized state after AD determines extent of synaptic recovery. **(A–C)** Graphs show measurements of synaptic response amplitudes before, during, and after anoxia with indicated delays between AD and re-oxygenation. A post-AD delay of 0 s before re-oxygenation **(A)** resulted in complete recovery, a delay of 120 s **(B)** yielded partial recovery, and a delay of 300 s **(C)** was followed by no recovery at all. Each point is the average of four consecutive responses, normalized to the pre-anoxia baseline period. The pink area denotes the anoxic period, and the insets represent synaptic responses recorded in the pre-anoxic (PRE), anoxic (ANOXIA), and recovery (POST) periods (each trace is an average of four consecutive trials). **(D)** Graph shows average (mean ± SEM) recovery of the synaptic response (percent of pre-anoxia baseline) in sets of slices tested with post-AD delays of 0 (n = 9), 30 (n = 9), 60 (n = 7), 90, (n = 5), 120 (n = 9), 180 (n = 10), and 300 (n = 8) s prior to re-oxygenation. Recovery was assessed 45 min after re-oxygenation. 100% recovery refers to the complete return of synaptic transmission, whereas 0% recovery refers to the complete of absence of evoked potentials. Experiments were conducted on B6 mice. The effect of re-oxygenation delay on recovery of synaptic transmission was highly significant (one-way Anova, $F_{6,50}$ = 15.06, p < 0.0001). *p < 0.05; ***p < 0.0001 (Dunnett's tests to compare indicated delays with delay = 0). (For interpretation of the references to colour in this figure legend, the reader is referred to the web version of this article.)

50 μM CNQX and 250 μM D-AP5 to block AMPA and NMDA receptors, respectively. After establishing a baseline recording for both synaptic and antidromic responses, the antagonist cocktail or sham drugs (vehicles) were administered for 40 min, followed by anoxia until AD occurred. The AD latency was recorded, and anoxia was continued for 2 min before re-oxygenation. Responses were monitored for at least 30 min of recovery. The results are presented for typical experiments using drug (Fig. 6A–C) or sham (Fig. 6D–F) treatment. As expected, sham-treated slices showed a suppression of synaptic transmission during anoxia, followed by the AD with coincident sudden loss of fiber volleys and antidromic responses and the appearance of AD waves with the dendritic wave slightly leading the somatic wave. In drug-treated slices, the synaptic response was completely antagonized by CNQX and D-AP5 without effect on antidromic responses; anoxia produced a delayed loss of antidromic responses coincident with the appearance of attenuated AD waves. The group data show that the glutamate antagonists significantly prolonged the AD latency (t_{18} = 5.57, p < 0.0001, Fig. 6G). The AD waves (recorded in *s. pyramidale*) in the drug-treated slices were also flattened compared to sham-treated slices, with amplitudes attenuated (t_{18} = 5.80, p < 0.0001, Fig. 6H) and duration increased (t_{18} = 3.46, p = 0.0028, Fig. 6I).

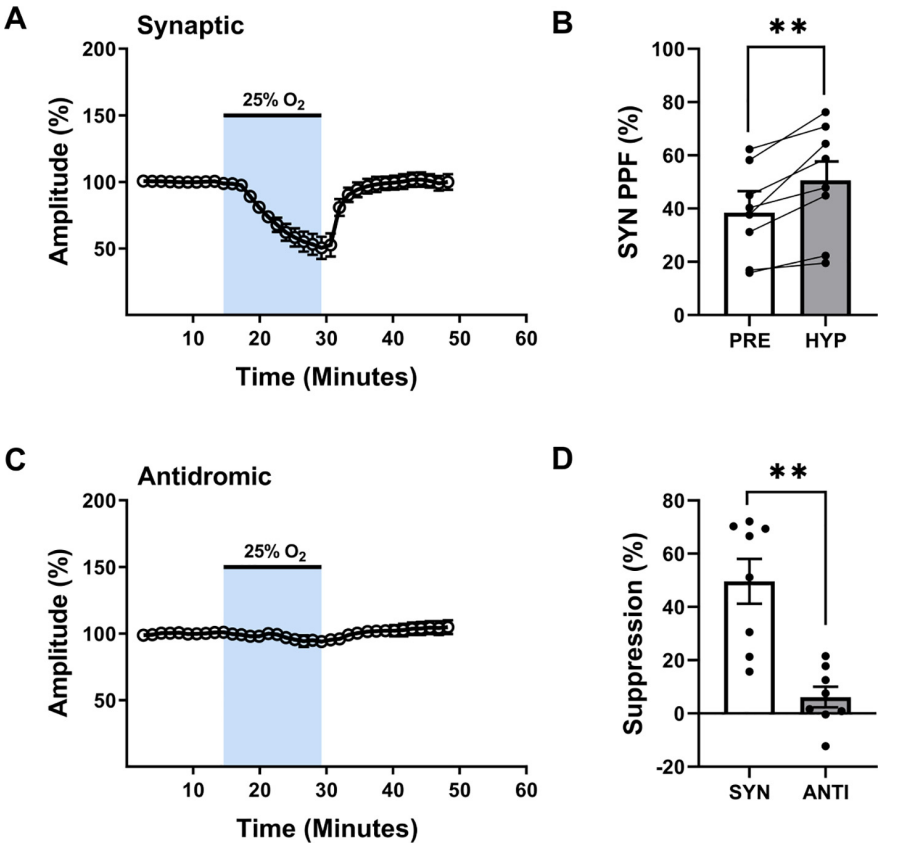

Fig. 3. Pre-synaptic suppression of synaptic transmission by partial hypoxia. **(A)** Averaged data from eight experiments show the effect of hypoxia on fEPSP amplitude. Each point is an average of four consecutive trials within each experiment, normalized to the baseline average, and averaged (mean ± SEM) across experiments at each time point. Hypoxia (25% O_2) was applied for 15 min (blue shaded area). Hypoxia caused a reduction in the amplitude of the fEPSP that was rapidly reversed upon return to normoxia. **(B)** Suppression of synaptic transmission in hypoxia was accompanied by an increase in paired-pulse facilitation (SYN PPF). Bars show the degree of PPF (75 ms IPI) immediately before (PRE) and at the end of the hypoxic period (HYP). SYN PPF was significantly enhanced in hypoxia (paired $t_7 = 4.50$, $p = 0.0028$; **). **(C)** Antidromic spikes were unaffected by hypoxia. Amplitudes of antidromic spikes were recorded during the same experiments in **(A)** and averaged in the same way. Hypoxia-induced suppression of synaptic amplitudes reached an average of 49.7% concomitant with a 4.7% reduction of antidromic spike amplitudes. **(D)** Synaptic responses were more affected by hypoxia than were antidromic spikes. Bars show that the suppression of fEPSPs (SYN) was significantly greater than the suppression of antidromic spikes (ANTI) during the hypoxic period (paired $t_7 = 4.92$, $p = 0.0017$; **).

AD propagation from CA3 shortens AD latency in CA1

The delay of AD by glutamate receptor antagonism suggests that the AD in CA1 may be propagated to CA1 from CA3 *via* the excitatory connections that remain intact in slice preparations. To test this, we measured AD latencies in CA3 and CA1 in slices in which the Schaffer collaterals connecting CA3 to CA1 were intact (Fig. 7A) or separated by a surgical cut (Fig. 7D). In intact slices, AD latencies in CA3 and CA1 were similar (Fig. 7B, C) whereas in slices with CA3/CA1 disconnection (CA1 deafferented), the AD latencies were much longer in CA1 than in CA3 (Fig. 7E, F). The data were analyzed by two-way analysis of variance, with slice condition (intact/disconnected) as a between-subjects variable and region (CA3/CA1) as a within-subjects variable. The analysis yielded a significant main effect of region ($F_{1,10} = 12.83$, $p = 0.0050$) and a significant interaction between region and slice condition ($F_{1,10} = 10.57$, $p = 0.0087$). Comparisons between AD latencies in CA3 and CA1 were significant for disconnected slices ($p = 0.0014$) but not for intact slices ($p = 0.97$; Sidak's test for multiple comparisons). Thus, it appears that CA1 neurons respond more slowly to anoxia when they have been deafferented from CA3. When those connections are intact, the earlier response to anoxia in CA3 is propagated to CA1.

To investigate this further, we conducted paired experiments in which CA1 responses to anoxia were recorded simultaneously in intact and disconnected (deafferented) slices (Fig. 8). Intact slices showed the early loss of synaptic transmission (due to adenosine release), followed by the appearance of the AD (Fig. 8A). In contrast, deafferented slices typically showed an initial suppression of synaptic transmission that corresponded to the suppression in intact slices but spontaneously recovered before falling again just prior to the occurrence of the AD (Fig. 8B). Responses of the intact and deafferented slices are shown overlain during the anoxic period in Fig. 8C and the AD latencies for all experiments are shown in Fig. 8D. AD latencies were significantly longer in deafferented slices compared to intact slices (paired $t_3 = 14.80$, $p = 0.0007$).

Antagonism of adenosine A_1 receptors in deafferented slices prolongs the maintenance of synaptic transmission during anoxia but has no effect on AD latency

The recovery of synaptic transmission after its initial suppression during the anoxic period has been occasionally noted in previous studies (Fowler, 1992); in our preparations it was only observed in deafferented slices. It seemed likely that the ablation of CA3 input uncovers the time course of adenosine action that is usually obscured by the propagation of early AD from CA3 to CA1. To test this, we recorded synaptic and antidromic responses during anoxia in deafferented slices after

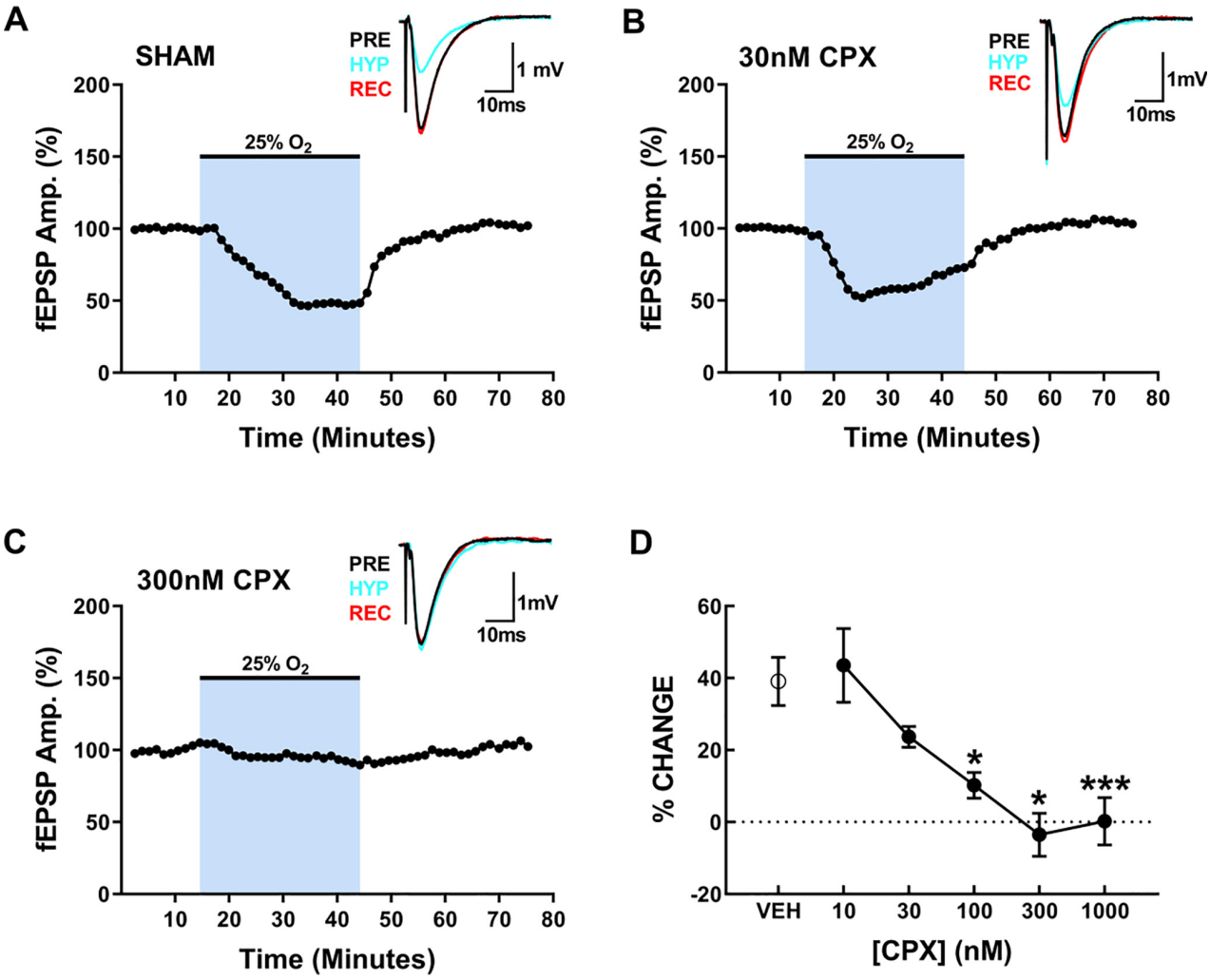

Fig. 4. Suppression of synaptic transmission by hypoxia is mediated by adenosine release and action on presynaptic A_1 receptors. **(A–C)** Representative experiments showing effects of a 30-min period of hypoxia (25% O_2) on synaptic responses in slices treated with vehicle (**(A)** Sham), 30 nM CPX **(B)**, or 300 nM CPX **(C)**. The blue area denotes the hypoxic period, and the insets represent individual synaptic responses for the pre-hypoxic (PRE), hypoxic (HYP), and recovery (REC) periods. **(D)** Group data showing % change in amplitude induced by hypoxia in slices treated with vehicle solution ($n = 20$) *versus* 10 nM ($n = 12$), 30 nM ($n = 6$), 100 nM ($n = 14$), 300 nM ($n = 4$), or 1000 nM ($n = 20$) CPX. Synaptic suppression showed a dose-dependent response to CPX with a threshold effect at 30 nM and complete maintenance of synaptic response at 300–1000 nM CPX (one-way Anova $F_{5,70} = 7.05$, $p < 0.0001$). *$p < 0.05$; ***$p < 0.001$ (Dunnett's tests for comparison of indicated dose with vehicle).

CPX or sham (vehicle) treatment (Fig. 9). Sham-treated slices showed the same pattern of change in synaptic response during anoxia as before: responses were suppressed early in the anoxic period, showed spontaneous recovery, and finally declined again until the AD occurred (Fig. 9A). In contrast, synaptic responses were maintained in CPX-treated slices until the decline leading to the AD (Fig. 9B). Antidromic responses in both sham- and CPX-treated slices were maintained until the rapid decline just prior to AD (Fig. 9D, E). The figure also shows the time course of anoxia effects on synaptic and antidromic responses superimposed during the anoxic period for Sham- (Fig. 9G) and for CPX- (Fig. 9H) treated slices. AD latencies measured at the appearance of depolarizing waves at the synaptic recording (Fig. 9C) or antidromic recording (Fig. 9F) sites showed no significant differences between sham- and CPX-treated slices.

Sex differences

Since men and women differ in stroke incidence and severity (Chauhan et al., 2017), we were interested to determine if responses to anoxia differed in slices from male and female mice. We measured AD latency in field CA1 of slices from 8-9 month old male and female B6 mice after nominal anoxia. Slices were either intact or deafferented (as in Fig. 7). Each slice was prepared for synaptic and antidromic stimulation and recording. For intact slices, AD latency did not differ significantly in slices from males and females (Fig. 10A). When comparisons were run using deafferented slices, however, slices from

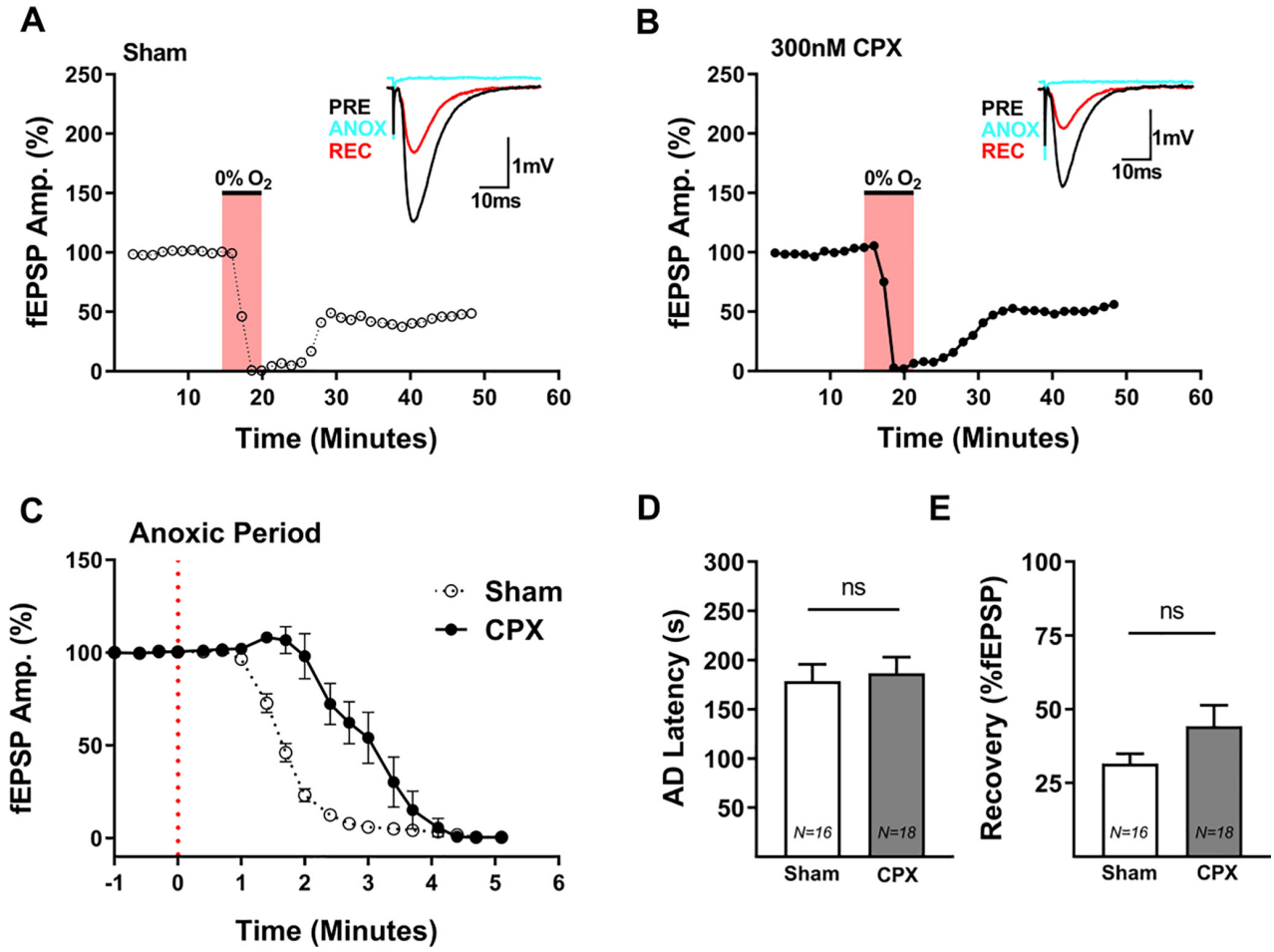

Fig. 5. Antagonism of adenosine A_1 receptors has no effect on AD latency or recovery of synaptic transmission after anoxia. **(A, B)** Representative experiments showing synaptic responses to anoxia after sham perfusion or administration of 300 nM CPX. Each point is an average of four consecutive trials. The sham-treated slice recorded an AD latency of 130 s while the CPX-treated slice recorded an AD latency of 142 s. The pink area denotes the anoxic period, and the insets represent synaptic responses (averages of four trials) for the pre-anoxic (PRE), anoxic (ANOX), and recovery (REC) periods in each condition. **(C)** Group data for sham (n = 32) and CPX (n = 30) conditions, highlighting the anoxic period (each point is an average of measurements of individual fEPSPs in all slices at each time-point). The abscissa is re-scaled relative to anoxia onset (vertical red-dotted line). **(D)** Histograms compare the AD latency (mean ± SEM) for sham- and CPX-treated slices (t_{32} = 0.33, p = 0.74). **(E)** Histograms compare post-anoxic recovery of fEPSPs at 30 min post-anoxia in sham- and CPX-treated slices (t_{32} = 1.54, p = 0.13). (For interpretation of the references to colour in this figure legend, the reader is referred to the web version of this article.)

female mice took significantly longer to reach AD than did slices from male mice (Fig. 10B).

DISCUSSION

The present study used the mouse hippocampal slice to investigate the steps in the ischemic cascade that contribute to the timing of AD. Clinically, the AD event is rapidly followed by the "early" cell death within the ischemic core; this differs from the "late" cell death taking place during reperfusion in the penumbra. This is an important distinction, because there are currently no treatments available to affect the ischemic core. Current interventions, whether preventative or rehabilitative, only attempt to treat the penumbra. As such, understanding the mechanisms that underlie the early-onset stages of ischemia (the "ischemic cascade"), and its spread from the core to the penumbra, would aid in the development of therapeutic modalities or pharmacology to ameliorate this rapid and deleterious event. Although the rapidity of AD within the ischemic core may preclude treatment in typical stroke patients, therapeutic measures may be possible to prevent extensive penumbra damage after stroke or to prevent AD in high-risk situations such as cardiac surgery.

In agreement with previous reports, we found that the time lapse between AD and re-oxygenation strongly influenced the degree of recovery of synaptic responsiveness: immediate re-oxygenation led to complete recovery, while a delay of more than 3 min was seldom followed by any recovery at all. The AD invariably involved three events that could be measured independently: (i) the abolition of the synaptic response and fiber volley, (ii) the loss of the AS, and (iii) the appearance of a large extracellularly-negative slow potential lasting 5–25 s, which we have termed the AD

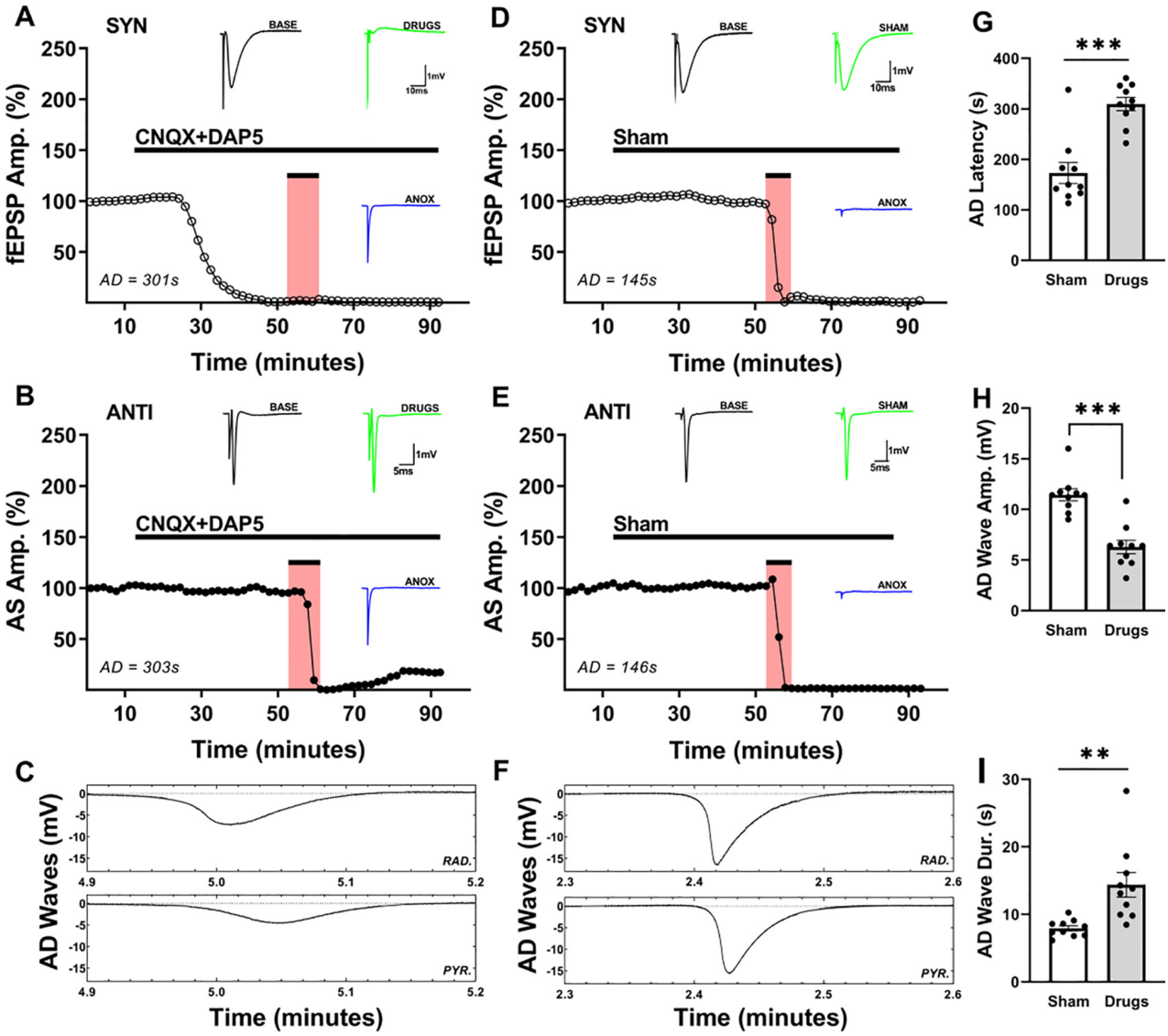

Fig. 6. Pharmacological antagonism of glutamate receptors extends AD latency. **(A–C)** Representative experiment showing synaptic and antidromic responses to anoxia after treatment with 50 μM CNQX and 250 μM D-AP5. The pink area represents the anoxic period and the insets show individual responses during baseline (BASE), drug application (DRUGS), and anoxia (ANOX). The synaptic response **(A)** was completely abolished by CNQX and DAP5, leaving only the fiber volley. The antidromic response **(B)** remained unaffected until its complete loss at AD. The elimination of the fiber volley and the antidromic response were coincident with the appearances of AD waves **(C)** in *s. radiatum* (RAD.) and *s. pyramidale* (PYR.), respectively. This drug-treated slice recorded an AD latency of 303 sec for the synaptic electrode and 305 sec for the antidromic electrode. **(D–F)** Representative experiment showing synaptic and antidromic responses to anoxia after sham treatment (CNQX vehicle: DMSO; D-AP5 vehicle: H_2O). The pink area represents the anoxic period and the insets show individual responses during baseline (BASE), vehicle perfusion (SHAM), and anoxia (ANOX). The synaptic response was maintained until becoming suppressed during anoxia, followed by AD with loss of the fiber volley and the antidromic response. The latencies to loss of the synaptic and antidromic responses were coincident with the appearances of the AD waves in *s. radiatum* (RAD.) and *s. pyramidale* (PYR.), respectively. This sham-treated slice recorded an AD latency of 146 sec for the synaptic electrode and 147 sec for the antidromic electrode. ***G –I,*** Bar graphs show the effect of glutamate antagonists on AD latency (t_{18} = 5.57, p < 0.0001; ***), AD wave amplitude (t_{18} = 5.80, p < 0.0001; ***), and AD wave duration (t_{18} = 3.46, p = 0.0028; **), compared to sham-treated slices. These measures were all taken at the antidromic recording site in *s. pyramidale*. (For interpretation of the references to colour in this figure legend, the reader is referred to the web version of this article.)

wave. The AD wave appears to be equivalent to the "DC shift" or "spreading depolarization" (or "spreading depression") used by other investigators (Aitken et al., 1988; Canals et al., 2008). Simultaneous recordings from dendritic and somatic zones allowed us to determine that the AD wave originates in the region of concentrated excitatory synapses and then propagates to the pyramidal cell layer.

The release of adenosine early in hypoxia or ischemia has been suggested as a neuroprotective mechanism (Rudolphi et al., 1992). It is well known that adenosine released into extracellular compartments inhibits synaptic

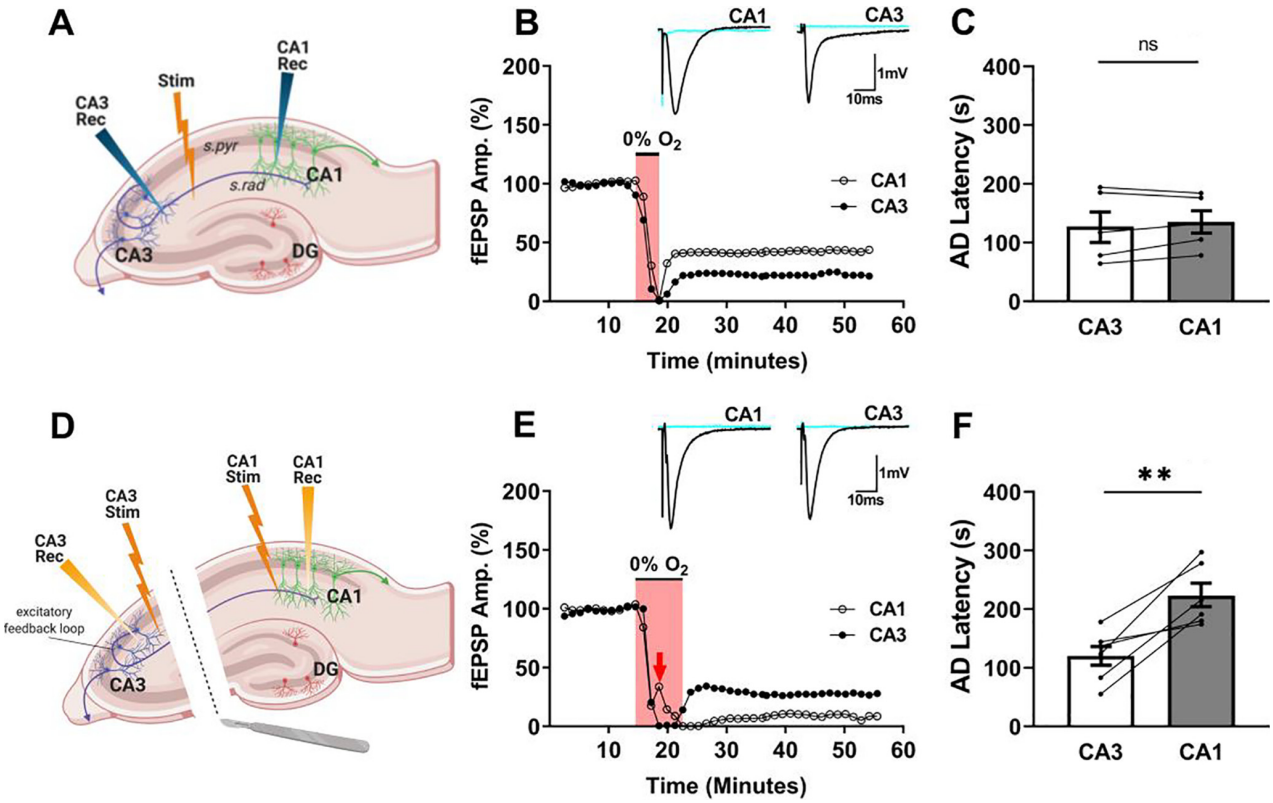

Fig. 7. AD is nearly simultaneous in CA3 and CA1 in intact slices but delayed in CA1, relative to CA3, in deafferented slices (CA1 disconnected from CA3). **(A)** Schematic showing the placement of simulating electrode (Stim) and recording electrodes in dendritic fields of CA1 (CA1 Rec) and CA3 (CA3 Rec) in an intact slice. **(B)** Representative experiment showing measurements of fEPSPs in CA1 (open circles) and CA3 (black circles) in response to anoxia (each point represents the average of four consecutive responses) in an intact slice. The pink area represents the anoxic period and the insets show averaged (n = 4) traces of synaptic responses in CA1 and CA3 for the baseline (black) and anoxic (blue) periods. This intact slice recorded an AD latency of 117 sec in CA3 and 132 sec in CA1. **(C)** Histograms compare AD latencies in CA1 and CA3 for intact slices. **(D)** Schematic showing the placement of simulating electrodes in CA1 (CA1 Stim) and CA3 (CA3 Stim) and recording electrodes in dendritic fields of CA1 (CA1 Rec) and CA3 (CA3 Rec) in a deafferented slice. **(E)** Representative disconnected slice experiment showing measurements of CA1 (open circles) and CA3 (black circles) fEPSPs in response to anoxia (each point represents the average of four consecutive responses). The pink area represents the anoxic period and the insets show averaged (n = 4) traces of synaptic responses in CA1 and CA3 for the baseline (black) and anoxic (blue) periods. This disconnected slice recorded an AD latency of 123 sec in CA3 and 297 sec in CA1. Note that the CA1 fEPSP displayed a transient, spontaneous recovery during the anoxic period (red arrow). **(F)** Histograms compare AD latencies in CA1 and CA3 for deafferented slices. $^{**}p < 0.01$. (For interpretation of the references to colour in this figure legend, the reader is referred to the web version of this article.)

release of glutamate (Dunwiddie and Masino, 2001) and that the suppression of synaptic transmission early in hypoxic challenge can be blocked by antagonists of A_1 receptors (Arlinghaus and Lee, 1996; Fowler, 1990; Kawamura et al., 2019; Tanaka et al., 2001). However, prior studies of the impact of released adenosine or its antagonism on the latency to AD produced conflicting results. Fowler (Fowler, 1990) first reported that 8-phenyltheophylline (8-PT) antagonized the loss of hippocampal CA1 synaptic responses during hypoxia in rat slices, but did not affect the time required for hypoxia-induced loss of the presynaptic fiber volley, a sign of AD. Similar observations were made by Oyama and colleagues (Oyama et al., 2020), measuring the AD latency in single neurons from slices from juvenile mice: AD latency was unaffected by administration of the A_1 antagonist, CPX. A study using rat slices also found no effect of the A_1 antagonist, 8-cyclopentyltheophylline (CPT), on ischemic depolarizations in single neurons (Tanaka et al., 2002). In contrast, Lee and Lowenkopf (1993) reported that the adenosine antagonists, theophylline and CPT, accelerated the appearance of AD in hippocampal slices from gerbils. On the other hand, Pearson and colleagues (Pearson et al., 2006) found that CPT blocked the AD induced by a brief hypoxic episode in CA1 of slices from neonatal rats, implying that blocking A_1 receptors delays the appearance of AD. Similarly, Fusco and colleagues (Fusco et al., 2018) found that antagonizing A_1 receptors with CPX delayed AD in CA1 of slices from adult rats. Beyond the A_1 receptor, selective antagonism of A_{2A} adenosine receptors significantly prevented or delayed the appearance of AD in dentate gyrus (DG) (Maraula et al., 2013) and CA1 (Pugliese et al., 2009) of rat hippocampal slices. Similar neuroprotective results were shown using selective antagonism of A_3 receptors in CA1 (Pugliese et al., 2006).

We verified that CPX blocks the suppression of synaptic transmission induced by hypoxia, both the steady-state suppression occurring during graded hypoxia and the early suppression in response to anoxic

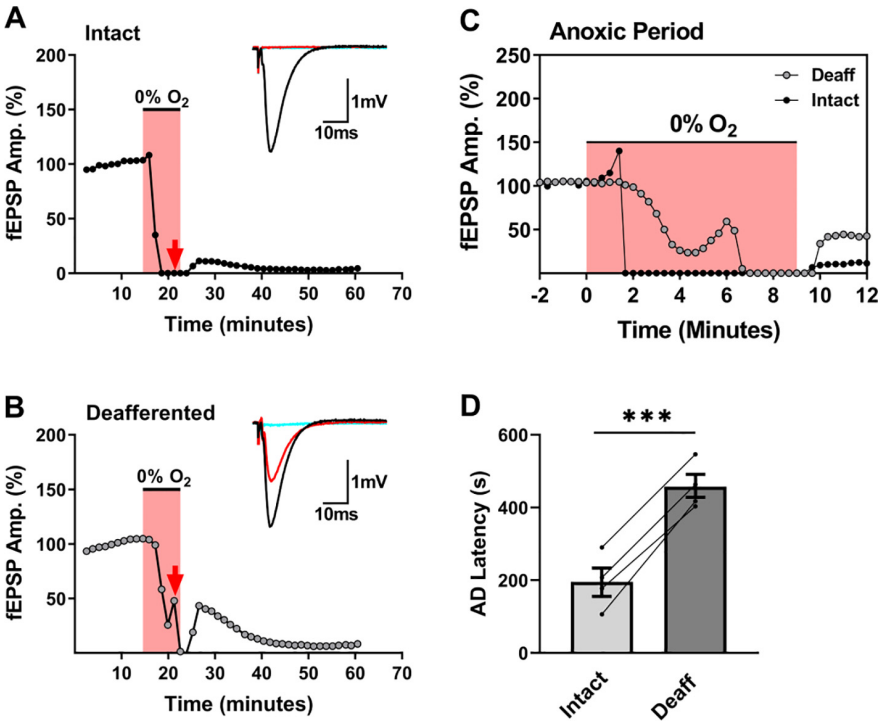

Fig. 8. Excitatory propagation from CA3 shortens AD latency in CA1. **(A, B)** Measurements of fEPSP amplitude in field CA1 of an intact slice **(A)** and a deafferented slice **(B)** in the same chamber before, during, and after an episode of anoxia (pink areas). Each point is an average of four consecutive trials. Insets show averaged traces (n = 4) collected during the baseline (black) and anoxic (blue) periods. Each red trace denotes averaged responses at the indicated timepoint (red arrow) and highlights the spontaneous recovery in the deafferented slice during the anoxic period. The AD latencies for the intact slice and deafferented slice were 106 s and 417 s, respectively. **(C)** Single-trial measurements from the same intact and deafferented slices with expanded time scale (relative to anoxia onset) to highlight the anoxic period. **(D)** Histograms comparing the AD latencies (mean ± SEM) for intact and deafferented slices in all paired experiments (paired t_3 = 14.80, p = 0.0007; ***). (For interpretation of the references to colour in this figure legend, the reader is referred to the web version of this article.)

challenge. In the latter case, however, the reinstatement of evoked glutamate release by CPX prior to AD had no significant effect on AD latency, either in intact slices or in slices in which the CA3 projections to CA1 were severed. We conclude that the adenosine-mediated suppression of synaptic glutamate release has very little impact on the occurrence of AD. Although the present data cannot rule out the potential effects of the nucleoside on other adenosine receptors within the hippocampal network (e.g. A_{2A-B} or A_3), our findings strongly suggest that A_1 receptors do not have a role in the latency to AD. Furthermore, these results may help to explain why genetic deletion of A_1 receptors does not alter the extent of damage after *in vivo* or *in vitro* ischemia (Olsson et al., 2004). That being said, Arrigoni and colleagues (Arrigoni et al., 2005) reported that deletion of A_1 receptors from CA3 neurons impaired recovery of synaptic transmission in CA1 neurons after hypoxic challenge, although it was not clear if or when AD occurred in those slices.

The role of glutamate excitotoxicity in ischemia-induced neuronal damage is well established: numerous studies have shown that antagonism of NMDA receptors attenuates cell damage and neuronal degeneration induced by hypoxia or ischemia *in vitro* and *in vivo* (Kass et al., 1989; Rothman et al., 1987; Wieloch, 1985). However, there are only a few studies examining the contribution of glutamate receptors to the timing of AD (Aitken et al., 1988; Fusco et al., 2018; Roberts et al., 1998; Tanaka et al., 1997; Yamamoto et al., 1997). We used two competitive antagonists, CNQX and D-AP5, at high doses to block AMPA and NMDA receptors, respectively, prior to anoxic challenge. The drugs blocked all evoked synaptic responses and significantly delayed the occurrence of AD. The drugs also significantly reduced the amplitude of the AD wave and extended its duration. Both of these effects may result from a decreased synchronization of the depolarizations occurring in individual neurons, although other mechanisms are possible.

The large increase in AD latency in slices in which glutamate receptors were blocked led us to examine whether the intact feed-forward glutamatergic connections from CA3 (the Schaffer collaterals) might contribute to the timing of AD in CA1. AD latency was found to be significantly longer in CA1 of slices in which the connections from CA3 were severed (CA1 deafferented) than in CA1 of intact slices. The delayed AD in CA1 of disconnected slices could arise from two types of mechanisms. First, the terminals of the severed Schaffer collaterals in CA1 may be less susceptible to anoxia than the intact axons, leading to a delay in the anoxia-dependent release of glutamate onto CA1 neurons in deafferented slices. This is consistent with the delayed AD in CA1 after blockade of glutamate receptors. Second, AD might be actively propagated from CA3 to CA1 in intact slices; disconnection would lead to a delay of the AD in CA1. The extensive excitatory feedback network within CA3 could favor a more rapid AD there in comparison to CA1 which has no such associational system (Amaral and Witter, 1989). Our finding of similar AD latencies in CA3 and CA1 in intact slices are consistent with this mechanism but are at odds with other data indicating a slower AD in CA3 than in CA1 after combined anoxia and hypoglycemia (Tanaka et al., 2002). Differences in experimental conditions might be responsible for this discrepancy.

The importance of isolating the local AD in CA1 from upstream CA3 influences was also evident in comparisons between male and female mice. AD

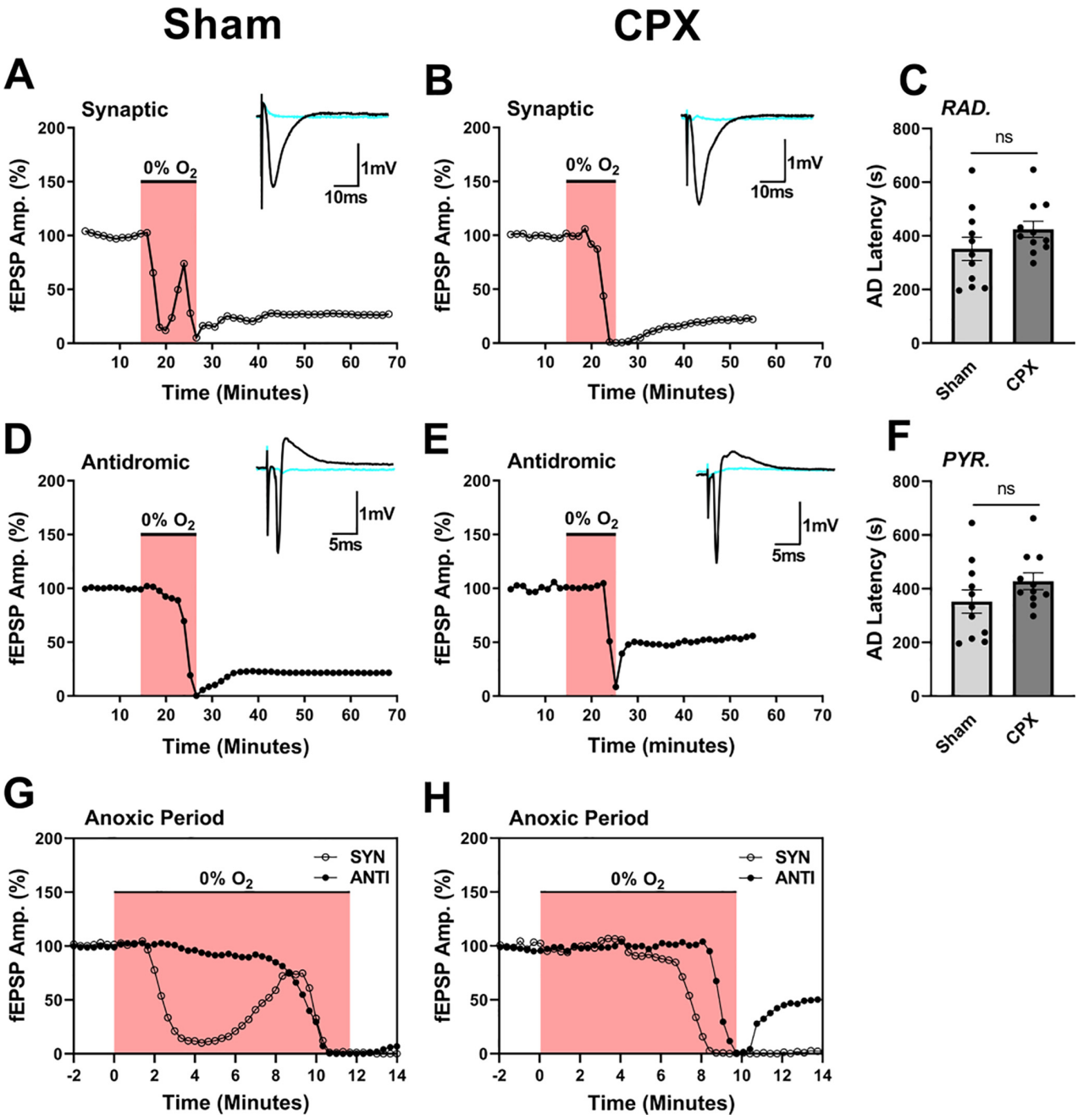

Fig. 9. CPX prolongs maintenance of synaptic transmission in deafferented slices during anoxia but does not affect AD latency. **(A, B)** Measurements of fEPSP amplitude in field CA1 of deafferented slices in experiments with continuous perfusion of sham vehicle **(A)** or 300 nM CPX **(B)** are shown before, during, and after an episode of anoxia (pink area). Each point represents the average of four trials and insets show averaged (n = 4) synaptic responses during the baseline (black) and anoxic (blue) periods. The AD latencies recorded in the dendritic field in these sham-treated and CPX-treated slices were 453 sec and 644 sec, respectively. **(C)** Histograms comparing AD latencies recorded in *s. radiatum* (*RAD.*) sham- and CPX-treated deafferented slices (t_{20} = 1.38, p = 0.18). **(D, E)** as in **(A, B)** but for antidromic spikes in the same two experiments. The AD latencies recorded in *s. pyramidale* were 457 sec for the sham slice and 645 sec for the CPX-treated slice. **(F)** as in **(C)**, but for AD waves recorded in the pyramidal (*PYR.*) cell layer (t_{20} = 1.42, p = 0.17). **(G, H)** Superimposed measurements of single-trial responses at expanded time scale (anoxia onset at t = 0) compare synaptic and antidromic responses from the same deafferented sham- **(G)** and CPX- **(H)** treated slices. CPX abolished the early suppression of synaptic transmission prior to AD. (For interpretation of the references to colour in this figure legend, the reader is referred to the web version of this article.)

latency in intact slices was not statistically different in males and females. However, in deafferented slices, the AD latency was significantly longer in females than in males. The mechanisms responsible are currently unclear. It has been previously reported that neuronal cultures prepared from neonatal female rats are less

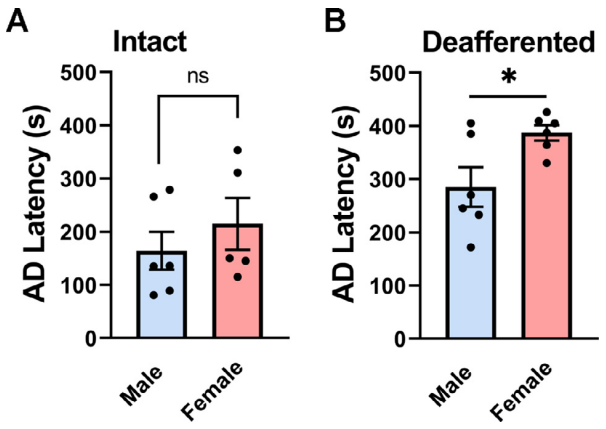

Fig. 10. Deafferentation of Schaffer Collateral pathway reveals AD differences between sexes. **(A)** Histograms comparing AD latencies (mean ± SEM) recorded in CA1 from intact male and female slices (male: 164.3 ± 35.5, female: 214.8 ± 48.7; $t_9 = 0.86$, $p = 0.41$) **(B)** Ablation of feedforward excitatory connections from CA3 to CA1 reveals longer AD latencies in females compared to males. Histograms compare AD latencies (mean ± SEM) recorded from CA1 in deafferented male and female slices (male: 285.0 ± 37.3, female: 386.8 ± 14.3; $t_{10} = 2.55$, $p = 0.029$; *).

susceptible to hypoxia-induced cell death than cultures from male animals. Future studies should aim to determine whether estrous cycle plays a potential role in these observed differences.

The results of the present investigations may aid in understanding adaptive mechanisms used by other vertebrate species that face chronic or intermittently hypoxic environmental conditions (Larson et al., 2014). For example, hippocampal slices from naked mole rats, animals that live in a chronically hypoxic habitat, show much longer latencies to AD than slices from mice tested under identical experimental conditions (Larson and Park, 2009). Further studies have shown that naked mole-rat hippocampus has an unusual complement of NMDA receptors and limited calcium uptake during hypoxic challenge (Peterson et al., 2012a, 2012b).

In summary, the studies described here have investigated synaptic and network properties that affect the timing of AD after oxygen deprivation in mouse hippocampal slices. This early electrophysiological event leads to the initiation of cell death cascades, and the latency of their occurrence provides strong predictive value for stroke outcome. Taken together, the results confirm glutamate as an important driver in the generation of AD during oxygen deprivation, and further delineate the neurotransmitter's action in the synaptic network. Antagonism of AMPA- and NMDA-type glutamate receptors significantly prolongs the latency to AD and alters the speed and synchrony of associated depolarizing waves. Although adenosine release during anoxia suppresses synaptic glutamate release via activation of presynaptic A_1 receptors, this event has no effect on AD latency or the potential for post-anoxic recovery of synaptic transmission. Importantly, we have shown that AD in field CA1 is significantly influenced by events upstream in the hippocampal trisynaptic circuit. Experiments using slices with fields CA3 and CA1 disconnected showed that AD latency is longer in CA1 of deafferented slices than in CA1 of intact slices. Deafferentation experiments also revealed that female mice display prolonged AD latencies in CA1 compared to male mice. Finally, our results confirm that the epoch between AD and re-oxygenation largely determines the magnitude of synaptic recovery after anoxic challenge. The longer neurons remain in the depolarized state, the more susceptible they become to the irreversible effects of AD. A comprehensive understanding of the cellular events leading to AD is important for the development of novel preventive strategies for stroke and other ischemic brain damage.

ACKNOWLEDGEMENTS

We thank Heba Akbari, Maribell Heredia, Sylvia Pawlowski, Uzma Saleha, Hanaa Siddiqi, and Yulianna Yaroshuk for assistance with some of the experiments.

FUNDING SOURCE

This work was supported by the National Science Foundation (IOS grants #0744979 and #1655494), The National Institutes of Health (HD084209), and the Campus Research Board of the University of Illinois at Chicago.

DECLARATIONS OF INTEREST

None.

REFERENCES

Aitken PG, Balestrino M, Somjen GG (1988) NMDA antagonists: lack of protective effect against hypoxic damage in CA1 region of hippocampal slices. Neurosci Lett 89:187–192.

Amaral DG, Witter MP (1989) The three-dimensional organization of the hippocampal formation: a review of anatomical data. Neuroscience 31:571–591.

Arai A, Larson J, Lynch G (1990) Anoxia reveals a vulnerable period in the development of long-term potentiation. Brain Res 511:353–357.

Arlinghaus L, Lee KS (1996) Endogenous adenosine mediates the sustained inhibition of excitatory synaptic transmission during moderate hypoxia. Brain Res 724:265–268.

Arrigoni E, Crocker AJ, Saper CB, Greene RW, Scammell TE (2005) Deletion of presynaptic adenosine A1 receptors impairs the recovery of synaptic transmission after hypoxia. Neuroscience 132:575–580.

Ayata C (2018) Monitoring anoxic depolarization at the bedside: A step closer to the 24th century. J Cereb Blood Flow Metab 38:1123–1124.

Balestrino M, Aitken PG, Somjen GG (1989) Spreading depression-like hypoxic depolarization in CA1 and fascia dentata of hippocampal slices: relationship to selective vulnerability. Brain Res 497:102–107.

Balestrino M, Somjen GG (1986) Chlorpromazine protects brain tissue in hypoxia by delaying spreading depression-mediated calcium influx. Brain Res 385:219–226.

Benjamin EJ, Virani SS, Callaway CW, Chamberlain AM, Chang AR, Cheng S, Chiuve SE, Cushman M, Delling FN, Deo R, de Ferranti SD, Ferguson JF, Fornage M, Gillespie C, Isasi CR, Jiménez MC, Jordan LC, Judd SE, Lackland D, Lichtman JH, Lisabeth L, Liu S, Longenecker CT, Lutsey PL, Mackey JS, Matchar DB, Matsushita

K, Mussolino ME, Nasir K, O'Flaherty M, Palaniappan LP, Pandey A, Pandey DK, Reeves MJ, Ritchey MD, Rodriguez CJ, Roth GA, Rosamond WD, Sampson UKA, Satou GM, Shah SH, Spartano NL, Tirschwell DL, Tsao CW, Voeks JH, Willey JZ, Wilkins JT, Wu JHY, Alger HM, Wong SS, Muntner P (2018) Heart disease and stroke statistics-2018 Update: A report from the American Heart Association. Circulation 137. https://doi.org/10.1161/CIR.0000000000000558.

Bickler PE, Zhan X, Fahlman CS (2005) Isoflurane preconditions hippocampal neurons against oxygen-glucose deprivation: role of intracellular Ca2+ and mitogen-activated protein kinase signaling. Anesthesiology 103:532–539.

Burke JF, Lisabeth LD, Brown DL, Reeves MJ, Morgenstern LB (2012) Determining stroke's rank as a cause of death using multicause mortality data. Stroke 43:2207–2211.

Canals S, Larrosa B, Pintor J, Mena MA, Herreras O (2008) Metabolic challenge to glia activates an adenosine-mediated safety mechanism that promotes neuronal survival by delaying the onset of spreading depression waves. J Cereb Blood Flow Metab 28:1835–1844.

Chauhan A, Moser H, McCullough LD (2017) Sex differences in ischaemic stroke: potential cellular mechanisms. Clin Sci (Lond) 131:533–552.

Coelho JE, de Mendonça A, Ribeiro JA (2000) Presynaptic inhibitory receptors mediate the depression of synaptic transmission upon hypoxia in rat hippocampal slices. Brain Res 869:158–165.

Croning MD, Haddad GG (1998) Comparison of brain slice chamber designs for investigations of oxygen deprivation in vitro. J Neurosci Methods 81:103–111.

Croning, M.D., Zetterstrom, T.S., Grahame-Smith, D.G., and Newberry, N.R. (1995). Action of adenosine receptor antagonists on hypoxia-induced effects in the rat hippocampus in vitro. Br J Pharmacol 116, 2113–2119.

Dunwiddie TV, Masino SA (2001) The role and regulation of adenosine in the central nervous system. Annu Rev Neurosci 24:31–55.

Fowler JC (1989) Adenosine antagonists delay hypoxia-induced depression of neuronal activity in hippocampal brain slice. Brain Res 490:378–384.

Fowler JC (1990) Adenosine antagonists alter the synaptic response to in vitro ischemia in the rat hippocampus. Brain Res 509:331–334.

Fowler JC (1992) Escape from inhibition of synaptic transmission during in vitro hypoxia and hypoglycemia in the hippocampus. Brain Res 573:169–173.

Fowler JC (1993) Changes in extracellular adenosine levels and population spike amplitude during graded hypoxia in the rat hippocampal slice. Naunyn Schmiedebergs Arch Pharmacol 347:73–78.

Fusco I, Ugolini F, Lana D, Coppi E, Dettori I, Gaviano L, Nosi D, Cherchi F, Pedata F, Giovannini MG, Pugliese AM (2018) The selective antagonism of adenosine A2B receptors reduces the synaptic failure and neuronal death induced by oxygen and glucose deprivation in rat CA1 hippocampus in vitro. Front Pharmacol 9:399.

Geiseler SJ, Larson J, Folkow LP (2016) Synaptic transmission despite severe hypoxia in hippocampal slices of the deep-diving hooded seal. Neuroscience 334:39–46.

Gundlfinger A, Bischofberger J, Johenning FW, Torvinen M, Schmitz D, Breustedt J (2007) Adenosine modulates transmission at the hippocampal mossy fibre synapse via direct inhibition of presynaptic calcium channels. J Physiol 582:263–277.

Hartings JA, Shuttleworth CW, Kirov SA, Ayata C, Hinzman JM, Foreman B, Andrew RD, Boutelle MG, Brennan KC, Carlson AP, et al. (2017) The continuum of spreading depolarizations in acute cortical lesion development: Examining Leao's legacy. J Cereb Blood Flow Metab 37:1571–1594.

Jarvis CR, Anderson TR, Andrew RD (2001) Anoxic depolarization mediates acute damage independent of glutamate in neocortical brain slices. Cereb Cortex 11:249–259.

Kaminogo M, Suyama K, Ichikura A, Onizuka M, Shibata S (1998) Anoxic depolarization determines ischemic brain injury. Neurol Res 20:343–348.

Kass IS, Chambers G, Cottrell JE (1989) The N-methyl-D-aspartate antagonists aminophosphonovaleric acid and MK-801 reduce anoxic damage to dentate granule and CA1 pyramidal cells in the rat hippocampal slice. Exp Neurol 103:116–122.

Kawamura M, Ruskin DN, Masino SA (2019) Adenosine A1 receptor-mediated protection of mouse hippocampal synaptic transmission against oxygen and/or glucose deprivation: a comparative study. J Neurophysiol 122:721–728.

Kostandy BB (2012) The role of glutamate in neuronal ischemic injury: the role of spark in fire. Neurol Sci 33:223–237.

Larson J, Drew KL, Folkow LP, Milton SL, Park TJ (2014) No oxygen? No problem! Intrinsic brain tolerance to hypoxia in vertebrates. J Exp Biol 217:1024–1039.

Larson J, Lynch G, Games D, Seubert P (1999) Alterations in synaptic transmission and long-term potentiation in hippocampal slices from young and aged PDAPP mice. Brain Res 840:23–35.

Larson J, Park TJ (2009) Extreme hypoxia tolerance of naked mole-rat brain. Neuroreport 20:1634–1637.

Leao AAP (1947) Further observations on the spreading depression of activity in the cerebral cortex. J Neurophysiol 10:409–414.

Lee KS, Lowenkopf T (1993) Endogenous adenosine delays the onset of hypoxic depolarization in the rat hippocampus in vitro via an action at A1 receptors. Brain Res 609:313–315.

Lipton P (1999) Ischemic cell death in brain neurons. Physiol Rev 79:1431–1568.

Maraula G, Traini C, Mello T, Coppi E, Galli A, Pedata F, Pugliese AM (2013) Effects of oxygen and glucose deprivation on synaptic transmission in rat dentate gyrus: role of A2A adenosine receptors. Neuropharmacology 67:511–520.

Olsson T, Cronberg T, Rytter A, Asztely F, Fredholm BB, Smith M-L, Wieloch T (2004) Deletion of the adenosine A1 receptor gene does not alter neuronal damage following ischaemia in vivo or in vitro. Eur J Neurosci 20:1197–1204.

Oyama Y, Ono K, Kawamura Jr M (2020) Mild hypothermia protects synaptic transmission from experimental ischemia through reduction in the function of nucleoside transporters in the mouse hippocampus. Neuropharmacology 163:107853.

Pearson T, Damian K, Lynas RE, Frenguelli BG (2006) Sustained elevation of extracellular adenosine and activation of A1 receptors underlie the post-ischaemic inhibition of neuronal function in rat hippocampus in vitro. J Neurochem 97:1357–1368.

Pérez-Pinzón MA, Mumford PL, Sick TJ (1998) Prolonged anoxic depolarization exacerbates NADH hyperoxidation and promotes poor electrical recovery after anoxia in hippocampal slices. Brain Res 786:165–170.

Peterson BL, Larson J, Buffenstein R, Park TJ, Fall CP, Nelson B (2012a) Blunted neuronal calcium response to hypoxia in naked mole-rat hippocampus. PloS ONE 7:e31568.

Peterson BL, Park TJ, Larson J (2012b) Adult naked mole-rat brain retains the NMDA receptor subunit GluN2D associated with hypoxia tolerance in neonatal mammals. Neurosci Lett 506:342–345.

Pugliese AM, Coppi E, Spalluto G, Corradetti R, Pedata F (2006) A3 adenosine receptor antagonists delay irreversible synaptic failure caused by oxygen and glucose deprivation in the rat CA1 hippocampus in vitro. Br J Pharmacol 147:524–532.

Pugliese AM, Traini C, Cipriani S, Gianfriddo M, Mello T, Giovannini MG, Galli A, Pedata F (2009) The adenosine A2A receptor antagonist ZM241385 enhances neuronal survival after oxygen-glucose deprivation in rat CA1 hippocampal slices. British journal of pharmacology 157, 818-830.

Roberts EL, Wisotzky D, Chih C-P (1998) Aging and the effects of MK-801 on anoxic damage in rat hippocampal slices. Brain Res 791:321–324.

Rossi DJ, Oshima T, Attwell D (2000) Glutamate release in severe brain ischaemia is mainly by reversed uptake. Nature 403:316–321.

Rothman SM, Thurston JH, Hauhart RE, Clark GD, Solomon JS (1987) Ketamine protects hippocampal neurons from anoxia in vitro. Neuroscience 21:673–678.

Rudolphi KA, Schubert P, Parkinson FE, Fredholm BB (1992) Neuroprotective role of adenosine in cerebral ischaemia. Trends Pharmacol Sci 13:439–445.

Schmidt-Kastner R, Freund TF (1991) Selective vulnerability of the hippocampus in brain ischemia. Neuroscience 40:599–636.

Schurr A, Reid KH, Tseng MT, West C, Rigor BM (1986) Adaptation of adult brain tissue to anoxia and hypoxia in vitro. Brain Res 374:244–248.

Tanaka E, Niiyama S, Uematsu K, Yokomizo Y, Higashi H (2002) The presynaptic modulation of glutamate release and the membrane dysfunction induced by in vitro ischemia in rat hippocampal CA1 neurons. Life Sci 72:363–374.

Tanaka E, Yamamoto S, Kudo Y, Mihara S, Higashi H (1997) Mechanisms underlying the rapid depolarization produced by deprivation of oxygen and glucose in rat hippocampal CA1 neurons in vitro. J Neurophysiol 78:891–902.

Tanaka E, Yasumoto S, Hattori G, Niiyama S, Matsuyama S, Higashi H (2001) Mechanisms underlying the depression of evoked fast EPSCs following in vitro ischemia in rat hippocampal CA1 neurons. J Neurophysiol 86:1095–1103.

Wieloch T (1985) Hypoglycemia-induced neuronal damage prevented by an N-methyl-D-aspartate antagonist. Science 230:681–683.

Yamamoto S, Tanaka E, Shoji Y, Kudo Y, Inokuchi H, Higashi H (1997) Factors that reverse the persistent depolarization produced by deprivation of oxygen and glucose in rat hippocampal CA1 neurons in vitro. J Neurophysiol 78:903–911.

(Received 26 October 2020, Accepted 16 February 2021)
(Available online 24 February 2021)